Steel and Composite Structures, *Vol. 33, No. 4* (*2019*) *473-487*
DOI: https://doi.org/10.12989/scs.2019.33.4.473

Shear-deformable finite element for free vibrations of laminated composite beams with arbitrary lay-up

Volkan Kahya*[1], Sebahat Karaca[1a] and Thuc P. Vo[2b]

[1] *Karadeniz Technical University*, *Faculty of Engineering*, *Department of Civil Engineering*, *61080 Trabzon*, *Turkey*
[2] *School of Engineering and Mathematical Sciences*, *La Trobe University*, *Bundoora*, *VIC 3086*, *Australia*

(*Received April 7, 2019, Revised October 5, 2019, Accepted October 30, 2019*)

Abstract. A shear-deformable finite element model (FEM) with five nodes and thirteen degrees of freedom (DOFs) for free vibrations of laminated composite beams with arbitrary lay-up is presented. This model can be capable of considering the elastic couplings among the extensional, bending and torsional deformations, and the Poisson's effect. Lagrange's principle is employed in derivation of the equations of motion, and thus the element matrices are obtained. Comparisons of the present element's results with those in experiment, available literature and the 3D finite element analysis software (ANSYS®) are made to show its accuracy. Some further results are given as referencing for the future studies in vibrations of laminated composite beamst.

Keywords: laminated composite beam; free vibration; finite element method; anisotropy

1. Introduction

Fibre reinforced composite materials have a wide range of applications in civil, mechanical, aerospace engineering and the related areas. The interest is due to their high strength, lightness, corrosion resistance, good thermal properties, design flexibility, etc. The mechanical behaviour of such materials under loading greatly depends on ply-stacking sequences. Due to anisotropic properties of composite materials, their structural analysis is more complicated than the metallic ones.

Since the laminated composite beams are often considered as important load-carrying elements of structures, an accurate model to predict their dynamic characteristics is necessary. In some cases, angle-ply and unsymmetric laminates may be essential from better design viewpoints. For angle-ply laminates, elastic couplings among extension, bending and torsion deformations due to anisotropy will become important. Furthermore, in one-dimensional analysis of laminated composites with no stresses in the width direction, neglecting the Poisson's effect causes the loss of some stiffness coefficients (Shao *et al*. 2017). Hence, the elastic couplings and the Poisson's effect should be considered in analysis of laminated composite beams with arbitrary lay-ups.

Various analytical and numerical models, which are based on various beam theories to consider the effect of shear deformation, rotary inertia, warping, and so forth, have been developed for laminated composite beams. A comprehensive literature review on their structural behaviours was summarized in Sayyad and Ghugal (2017). Among the solution methods, the finite element method (FEM) has been widely used by researchers due to its flexibility to define the unknown displacement variables by various polynomial expressions. In literature, various finite element models based on the first-order/Timoshenko and higher-order as well as layer-wise and zig-zag beam theories for the free vibration analysis of laminated composite and sandwich beams have been developed. Some papers related to each theory are briefly summarized in the following separate paragraphs.

Based on the first-order beam theory, Kadivar and Mohebpour (1998) proposed a beam element having 16, 20 and 24 degrees of freedom (DOFs) for dynamic analysis of unsymmetric laminated composite beams subjected to moving loads. Chakraborty *et al*. (2002) developed a refined locking-free beam element for free vibration and wave propagation analyses of asymmetric laminated composite beams. Goyal and Kapania (2007) developed a 21-DOF beam element for analysis of laminated composite beams with arbitrary lay-ups, in which an accurate model for the shear correction factor was used. Jun *et al*. (2008) derived a dynamic FEM, which incorporated the Poisson's effect and couplings among extensional, flexural and torsional deformations, to perform free vibration analysis of generally laminated composite beams. Mohebpour *et al*. (2011) studied the dynamic response of laminated composite beams under the action of a moving oscillator. They accounted for the complete dynamic interaction between the beam and oscillator. Kahya (2012) studied the dynamic response of laminated composite beams subjected to moving loads by using a multi-layered finite element. This model considered separate rotational DOFs for each lamina but did not require any additional axial or transversal DOFs. Jafari-Talookolaei *et al*. (2017) proposed

*Corresponding author, Professor,
E-mail: volkan@ktu.edu.tr
[a] Ph.D. Candidate
[b] Associate Professor

http://www.techno-press.org/?journal=scs&subpage=6 ISSN: 1229-9367 (Print), 1598-6233 (Online)

a FEM for in-plane and out-of-plane vibrations of laminated composite beams. They indicated the importance of out-of-plane displacement component in calculation of torsional modes.

Based on higher-order beam theories, Shi and Lam (1999) developed a two-noded beam element for free vibration of laminated composite beams. They studied the effect of mass components due to the higher-order displacement and the coupling of the different order axial displacement components on the accuracy of analysis. Subramanian (2006) presented the free vibration analysis of laminated composite beams by two-noded C^1 beam elements. In-plane and out-of-plane displacements were, respectively, assumed as a quantic and quartic variation through-the-thickness. Lezgy-Nazargah *et al*. (2011) developed a refined high-order global-local theory for laminated and sandwich beams, that satisfies all the kinematic and stress continuity conditions at the layer interfaces and considers the effects of transverse normal stress and transverse flexibility. Vo and co-workers proposed a two-noded beam element for vibration and buckling of laminated composite beams with arbitrary lay-ups (Vo and Thai 2012a, b, Vo *et al*. 2013). They took into account the parabolical and sinusoidal variation of shear strains through-the-thickness. Later, they included both shear and normal deformations to study free vibrations of composite beams with axial loads (Vo *et al*. 2017).

This paragraph reviews few papers related to layer-wise and zig-zag beam theories for free vibrations of laminated composite beams. Ramtekkar *et al*. (2002) developed a six-noded, plane-stress mixed FEM by using Hamilton's principle. Vidal and Polit (2010) proposed a family of sinus models for the free vibration analysis of laminated composite beams. Chalak *et al*. (2012) investigated the free vibration of soft-core sandwich beams using a C^0 beam element based on a higher-order zig-zag theory, in which the cubic and quadratic distribution of axial and transverse displacement were considered. Filippi and Carrera (2016) proposed 1D layer-wise theories using the higher-order zig-zag functions defined over fictitious/mathematical layers of the cross-sectional area. Wimmer and Gherlone (2017) presented explicit expressions for the linear and geometric stiffness matrix, the mass matrix and the equivalent nodal force vector of a simple planar beam element based on the refined zig-zag theory. Kahya and Turan (2018) presented a multilayer finite element for buckling and free vibration of laminated composite and sandwich beams based on a higher-order layer-wise theory. They gave some comparisons for buckling loads and natural frequencies of beams with different end conditions and lamina stacking to show the accuracy of proposed element.

Although the elastic couplings due to anisotropy and the Poisson's effect are well-studied in laminated composite beams by various analytical/semi-analytical methods, according to above-given literature survey, the numerical solutions based on FEM accounting for both bending-extension, bending-twist and extension-twist couplings and the Poisson's effect in free vibrations of such structural elements has not been adequately studied. To fill this gap, we proposed a five-noded finite element with 13 DOFs based on the first-order shear deformation theory. This higher-order element is capable of considering the aforementioned couplings due to anisotropy and the Poisson's effect. By using Lagrange's principle, governing equations of motion and the element mass and stiffness matrices are derived. Natural frequencies and corresponding mode shapes of laminated composite beams are then obtained by solving the standard eigenvalue problem under various boundary conditions, lay-ups, orthotropy ratio and slenderness. In order to show accuracy of the present element, comparisons with the experimental study, available literature and finite element analyses in ANSYS® (2014) are made. Some numerical results are presented for the first time as a reference for the future studies in the area.

2. Governing equations of motion

A laminated composite beam of length L, width b and height h is considered as illustrated in Fig. 1. The beam is made of n orthotropic layers with different fibre angle measured in counter-clockwise direction to the x-axis.

Based on the first-order beam theory, the displacement field can be assumed as

$$\begin{aligned} u(x,z,t) &= u_0(x,t) + z\theta(x,t), \\ v(x,z,t) &= z\psi(x,t), \\ w(x,z,t) &= w_0(x,t) \end{aligned} \tag{1}$$

where u, v and w are the displacement components in the x-, y- and z-directions at any point of the beam, respectively. u_0 and w_0 are the displacements in the x- and z-directions at a point on the midplane, θ and ψ are the rotations of the normal to the midplane about the y- and x-axes, respectively, and t is time. The displacement field in Eq. (1) allows that the beam can stretch along the z-axis, bend in the x-z plane, and twist around x-axis. Note that there is no bending in the y-z plane. With the use of such displacement field, one can take into account the bending-stretching, bending-torsion and torsion-stretching couplings due to anisotropy in the formulation. The displacement field given by Eq. (1) has been previously used by Jun *et al*. (2008) and Jafari-Talookolaei *et al*. (2012) for the free vibration analysis of generally laminated composite beams, by Mohebpour *et al*. (2011) for the dynamic response analysis

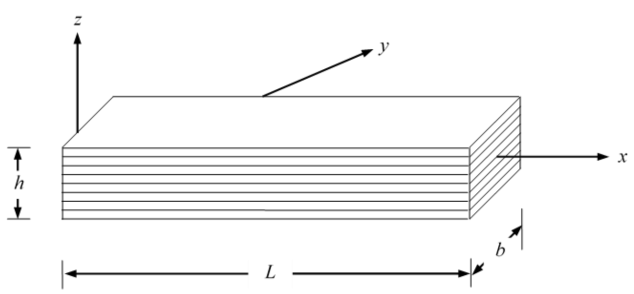

Fig. 1 Geometry and coordinate system for laminated composite beam with rectangular cross-section

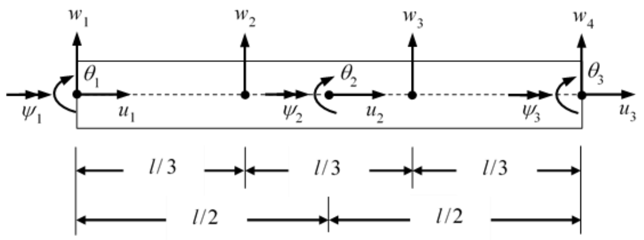

Fig. 2 13-DOF beam finite element

of laminated beams subjected to moving oscillators, and by Wang *et al*. (2015) for the buckling analysis of laminated composite beams with general lamina layup. For the present study, the displacement field given by Eq. (1) is used to develop a higher-order finite element for laminated composite beams shown in Fig. 2.

From Eq. (1), the strain-displacement relationships can be written as follows

$$\begin{aligned} \varepsilon_x &= u_{,x} = \varepsilon_x^0 + z\kappa_x, \\ \gamma_{xz} &= u_{,z} + w_{,x} = w_{0,x} + \theta, \\ \gamma_{xy} &= u_{,y} + v_{,x} = z\kappa_{xy} \end{aligned} \tag{2}$$

where $\varepsilon_x^0 = u_{0,x}$, $\kappa_x = \theta_{,x}$ and $\kappa_{xy} = \psi_{,x}$ are the midplane strain, bending and twisting curvatures, respectively, (,x) denotes the derivative with respect to x.

The constitutive relations of the laminate can be given by (Reddy 1997)

$$\begin{Bmatrix} N_x \\ N_y \\ N_{xy} \\ M_x \\ M_y \\ M_{xy} \end{Bmatrix} = \begin{bmatrix} A_{11} & A_{12} & A_{16} & B_{11} & B_{12} & B_{16} \\ A_{12} & A_{22} & A_{26} & B_{12} & B_{22} & B_{26} \\ A_{16} & A_{26} & A_{66} & B_{16} & B_{26} & B_{66} \\ B_{11} & B_{12} & B_{16} & D_{11} & D_{12} & D_{16} \\ B_{12} & B_{22} & B_{26} & D_{12} & D_{22} & D_{26} \\ B_{16} & B_{26} & B_{66} & D_{16} & D_{26} & D_{66} \end{bmatrix} \begin{Bmatrix} \varepsilon_x^0 \\ \varepsilon_y^0 \\ \gamma_{xy} \\ \kappa_x \\ \kappa_y \\ \kappa_{xy} \end{Bmatrix} \tag{3}$$

$$\begin{Bmatrix} Q_{yz} \\ Q_{xz} \end{Bmatrix} = \begin{bmatrix} A_{44} & A_{45} \\ A_{45} & A_{55} \end{bmatrix} \begin{Bmatrix} \gamma_{yz} \\ \gamma_{xz} \end{Bmatrix} \tag{4}$$

where N_x, N_y and N_{xy} are the in-plane forces, M_x, M_y and M_{xy} are the bending and twisting moments, Q_{yz} and Q_{xz} are the transverse shear forces per unit length, ε_x^0, ε_y^0, and γ_{xy} are the normal and shear strains, κ_x, κ_y and κ_{xy} are the bending and twisting curvatures, respectively. The laminate stiffness coefficients A, B and D are given by

$$\begin{aligned} (A_{ij}, B_{ij}, D_{ij}) &= \sum_{k=1}^{n} \int_{z^k}^{z^{k+1}} \bar{Q}_{ij}^k (1, z, z^2) dz \quad (i = j = 1,2,6), \\ A_{ij} &= \sum_{k=1}^{n} K \int_{z^k}^{z^{k+1}} \bar{Q}_{ij}^k dz \quad (i = j = 4,5) \end{aligned} \tag{5}$$

where K is the shear correction factor, n is the number of layers in the laminate, and $\bar{Q}_{ij}^k$ are the transformed reduced stiffness constants for the kth layer obtained by considering the transverse normal stress σ_z be negligible. They can be found in the explicit form in Reddy (1997).

To include the Poisson's effect, the strain components ε_y^0 and γ_{yz}, and the curvature κ_y are assumed as non-zero while the in-plane forces N_y and N_{xy}, the bending moment M_y and the lateral shearing force Q_{yz} are equal to zero. Therefore, Eqs. (3) and (4) can be rewritten as

$$\begin{Bmatrix} N_x \\ M_x \\ M_{xy} \end{Bmatrix} = \begin{bmatrix} \bar{A}_{11} & \bar{B}_{11} & \bar{B}_{16} \\ \bar{B}_{11} & \bar{D}_{11} & \bar{D}_{16} \\ \bar{B}_{16} & \bar{D}_{16} & \bar{D}_{66} \end{bmatrix} \begin{Bmatrix} \varepsilon_x^0 \\ \kappa_x \\ \kappa_{xy} \end{Bmatrix} \tag{6}$$

$$Q_{xz} = \bar{A}_{55} \gamma_{xz} \tag{7}$$

where

$$\begin{aligned} \begin{bmatrix} \bar{A}_{11} & \bar{B}_{11} & \bar{B}_{16} \\ \bar{B}_{11} & \bar{D}_{11} & \bar{D}_{16} \\ \bar{B}_{16} & \bar{D}_{16} & \bar{D}_{66} \end{bmatrix} &= \begin{bmatrix} A_{11} & B_{11} & B_{16} \\ B_{11} & D_{11} & D_{16} \\ B_{16} & D_{16} & D_{66} \end{bmatrix} - \begin{bmatrix} A_{12} & A_{16} & B_{12} \\ B_{12} & B_{16} & D_{12} \\ B_{26} & B_{66} & D_{26} \end{bmatrix} \times \\ &\times \begin{bmatrix} A_{22} & A_{26} & B_{22} \\ A_{26} & A_{66} & B_{26} \\ B_{22} & B_{26} & D_{22} \end{bmatrix}^{-1} \begin{bmatrix} A_{12} & A_{16} & B_{12} \\ B_{12} & B_{16} & D_{12} \\ B_{26} & B_{66} & D_{26} \end{bmatrix}^{\mathrm{T}} \end{aligned} \tag{8}$$

$$\bar{A}_{55} = A_{55} - \frac{A_{45}^2}{A_{44}} \tag{9}$$

Eqs. (6) and (7) are the constitutive relations for a laminated composite beam including the Poisson's effect. The coefficients $\bar{A}$, $\bar{B}$ and $\bar{D}$ are replaced by A, B and D to ignore this effect.

The strain energy U of the system is

$$U = \frac{1}{2} \int_0^L \left[N_x \varepsilon_x^0 + M_x \kappa_x + M_{xy} \kappa_{xy} + Q_{xz} \gamma_{xz} \right] b dx \tag{10}$$

Substituting Eqs. (2), (6) and (7) into Eq. (10) yields

$$\begin{aligned} U = \frac{1}{2} \int_0^L \Big[& \bar{A}_{11} u_{0,x}^2 + 2\bar{B}_{11} u_{0,x} \theta_{,x} + 2\bar{B}_{16} u_{0,x} \psi_{,x} \\ & + \bar{D}_{11} \theta_{,x}^2 + 2\bar{D}_{16} \theta_{,x} \psi_{,x} + \bar{D}_{66} \psi_{,x}^2 + \bar{A}_{55} (w_{0,x} + \theta)^2 \Big] b dx \end{aligned} \tag{11}$$

The kinetic energy T of system is

$$T = \frac{1}{2} \int_0^L \int_{-h/2}^{h/2} \rho (\ddot{u}^2 + \ddot{v}^2 + \ddot{w}^2) b dz \, dx \tag{12}$$

where ρ is the mass density, and dot denotes the derivative with respect to time. Substituting Eqs. (1) into Eq. (12) and performing integration with respect to z yields

$$T = \frac{1}{2} \int_0^L \left[I_0 (\dot{u}_0^2 + \dot{w}_0^2) + 2 I_1 \dot{u}_0 \dot{\theta} + I_2 (\dot{\theta}^2 + \dot{\psi}^2) \right] b dx \tag{13}$$

where

$$(I_0, I_1, I_2) = \sum_{k=1}^{n} \int_{z^k}^{z^{k+1}} \rho (1, z, z^2) dz \tag{14}$$

By using the Lagrange's principle given by

$$\frac{d}{dt}\left[\frac{\partial L}{\partial \dot{q}_i}\right]-\frac{\partial L}{\partial q_i}=0 \tag{15}$$

where $L = T - U$ is the Lagrangian functional and q denotes the unknown variables u_0, w_0, θ and ψ, the governing equations of motion for the laminated composite beam can be derived.

3. Finite element model

The present finite element has five nodes and thirteen DOFs as shown in Fig. 2. The element can be capable of taking into account the shear deformation, rotary inertia, Poisson's effect and elastic couplings due to anisotropy. The additional DOFs at the inner nodes provides to better represent the complex behaviour of the generally layered composite beams.

The solutions are assumed to be

$$\begin{aligned} u_0 &= \sum_{i=1}^{3} \Phi_i(x)\, u_i(t), \quad w_0 = \sum_{i=1}^{4} \Psi_i(x)\, w_i(t), \\ \theta &= \sum_{i=1}^{3} \Phi_i(x)\, \theta_i(t), \quad \psi = \sum_{i=1}^{3} \Phi_i(x)\, \psi_i(t) \end{aligned} \tag{16}$$

where $\Phi_i(x)$ and $\Psi_i(x)$ are, respectively, quadratic and cubic Langrange polynomials. According to Eq. (2), the axial deformation is dependent on first spatial derivatives of u_0 and θ. Thus, the degree of polynomials of u_0 and θ must be same. Also, the shear strain γ_{xz} is a linear function of $w_{0,x}$ and θ, thus the degree of polynomial used for w_0 must be one order higher than those used for u_0 and θ to ensure compatibility. Therefore, the cubic polynomial used for w_0 requires that quadratic functions for both u_0 and θ for consistency. Such choice also prevents the shear locking. In addition, the quadratic polynomial for ψ is appropriate since the twisting DOFs are located at the same nodes with extensional and rotational DOFs. Explicit expressions of the shape functions are given in Appendix.

The solutions given by Eq. (16) are substituted into the energy expressions given by Eqs. (11) and (13), the result is substituted into Eq. (15), after some arrangements, the following expression can be obtained

$$\boldsymbol{M}_e \ddot{\boldsymbol{u}}_e + \boldsymbol{K}_e \boldsymbol{u}_e = \boldsymbol{0} \tag{17}$$

where $\mathbf{M_e}$ and $\mathbf{K_e}$ are the element mass and stiffness matrices and $\mathbf{u_e}$ is a vector including the nodal displacements, respectively, which are given in Appendix.

The element matrices are assembled into the global ones such as $\boldsymbol{M}_{(9m+4)\times(9m+4)}$ and $\boldsymbol{K}_{(9m+4)\times(9m+4)}$, where m is the number of elements. Thus, the total number of nodal displacements in the discretized finite element model of the beam is $(9m + 4)$. The global matrix equation of motion for free vibrations of the whole system becomes

$$\boldsymbol{M}\ddot{\boldsymbol{U}} + \boldsymbol{K}\boldsymbol{U} = \boldsymbol{0} \tag{18}$$

where $\mathbf{M}$ and $\mathbf{K}$ are the global mass and stiffness matrices, and $\mathbf{U}$ is the nodal displacements of the entire system. Assuming the solution of Eq. (18) to be in the form $\boldsymbol{U} = \boldsymbol{U}_0 e^{i\omega t}$ yields

$$(\boldsymbol{K} - \omega^2 \boldsymbol{M})\boldsymbol{U}_0 = \boldsymbol{0} \tag{19}$$

where ω is the natural frequency, U_0 is the mode shapes vector. The nontrivial solution of Eq. (19) requires solving the standard eigenvalue problem as $det(\boldsymbol{K} - \omega^2\boldsymbol{M}) = 0$ for the natural frequencies. The corresponding mode shapes can then be obtained by Eq. (19) with back-substituting.

4. Results and discussion

Results for natural frequencies and mode shapes of the laminated composite beams with various configurations including boundary conditions and lay-ups are presented in this section. Comparisons with the experimental study, available literature and the finite element analyses in ANSYS® are made to show the accuracy, reliability and feasibility of the present element. Further, some new results, which may be used as reference data for future, are

Table 1 Convergence study of the present element for a clamped-clamped laminated beam with $[30/50]_2$ lay-up

Number of elements (m)	Natural frequencies (Hz)				
	1st mode	2nd mode	3rd mode	4th mode	5th mode
2	647.416	2059.921	3927.237	5104.989	5385.672
4	638.749	1660.087	3052.057	3913.302	5061.198
8	638.036	1648.654	3005.153	3911.176	4605.382
12	637.997	1647.981	3001.087	3911.058	4591.068
16	637.991	1647.866	3000.383	3911.038	4588.517
20	**637.989**	**1647.835**	**3000.188**	**3911.032**	**4587.807**
24	637.988	1647.824	3000.118	3911.030	4587.550
30	637.988	1647.817	3000.079	3911.029	4587.408
Jun *et al*. (2008)	637.9	1647.8	3000.0	3911.0	4587.3

presented. In numerical examples, the shear correction factor K is taken to be 5/6, and all layers within the laminate is assumed to have equal thickness. Five boundary conditions are considered such as clamped-clamped (C-C), simply supported (S-S), clamped-free (C-F), clamped-simply supported (C-S) and free-free (F-F) at its both ends of laminated composite beams.

4.1 Convergence study

A convergence study is performed to determine the number of elements that will be sufficient in the numerical examples. To this aim, an unsymmetric $[30/50]_2$ laminated composite beam with clamped-clamped end conditions is considered. Geometry and material properties of the beam are E_1 = 144.8 GPa, E_2 = 9.65 GPa, G_{12} = G_{13} = 4.14 GPa, G_{23} = 3.45 GPa, ν = 0.3, ρ = 1389.23 kg/m^3, L = 0.381 m, b = h = 25.4 mm. The first five natural frequencies (in Hz) for bending vibrations of the laminated composite beam are presented in Table 1 with various number of elements along with the analytical results given by Jun *et al*. (2008). As can be seen, a rapid convergence is obtained, and m = 20 elements are sufficient to guarantee the numerical convergence. Besides, an excellent agreement with the analytical results given by Jun *et al*. (2008) can be observed.

Fig. 3 The laboratory model of the cantilever composite beam for experimental measurements

4.2 Verification with experimental result

In this study, the ambient vibration test of a cantilever composite beam with the lamination scheme of [90/±45/0/90/±45/0/±45/90] is carried out. The test beam has the length L = 1 m, width b = 80 mm, thickness h = 8 mm. The material properties are given by E_1 = 30.6 GPa, E_2 = 8.5 GPa, G_{12} = G_{13} = G_{23} = 3.26 GPa, ν_{12} = 0.34, ρ = 1920 kg/m^3.

B&K3560 data acquisition system with 17 channels, B&K8340-type uniaxial accelerometers and uniaxial signal cables are used in measurements. Recording data is processed in PULSE (2006) and OMA (2006) software for extracting the dynamic characteristics. Ten sensitive accelerometers are located on the beam in vertical direction shown in Fig. 3, and measurements are performed during 10 minutes. Frequency span, FFT analysers and multi-buffer are 0-128 Hz, 800 lines and 100 averages, 50 size and 500 m update, respectively. Enhanced Frequency Domain Decomposition (EFDD) method and Stochastic Subspace Identification (SSI) method are used to obtain the modal characteristics. Singular values of spectral density matrices (SVSDM) and the average of auto spectral densities (AASD) of data set obtained by EFDD method, stabilization diagram of estimated state space models and select-link modes across data sets obtained by SSI method are shown in Fig. 4 for undamaged beam. The peaks of the curves in the figures indicate the natural frequencies.

Experimental results are compared with those calculated by the present model and ANSYS® in Table 2. In the ANSYS® modelling, SHELL181 element which allows for layered shell definition is used. SHELL181 is a four-node element with six DOFs at each node: translations in the x-, y-, and z-directions, and rotations about the x-, y-, and z-axes (see Fig. 5), and is capable of specifying the thickness,

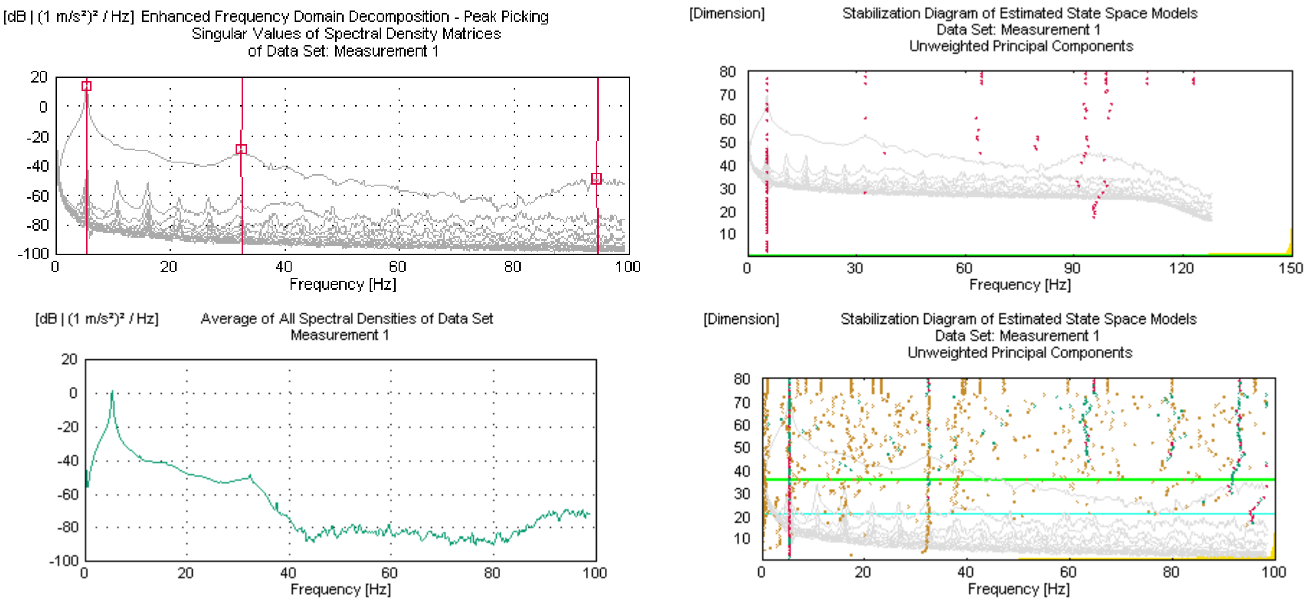

Fig. 4 EFDD and SSI results for undamaged beam

Table 2 Comparison of natural frequencies (in Hz) for in-plane bending vibrations of a cantilever laminated beam with experiment

Mode	Experimental	ANSYS®	Present model	
			Poisson's effect excluded	Poisson's effect included
1	5.37	5.1664	5.1075	5.1933
2	32.52	32.5517	31.9799	32.5158
3	96.64	90.5035	89.4149	90.9090

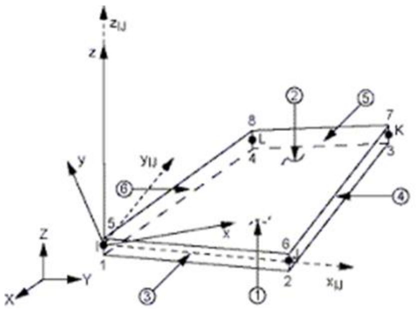

Fig. 5 SHELL181 element geometry

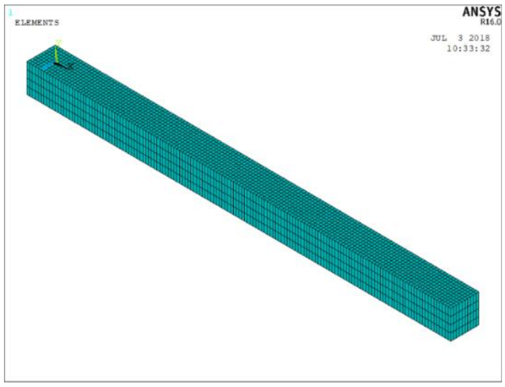

Fig. 6 Representative FE model of a laminated composite beam in ANSYS®

material, fibre orientation and the number of integration points through the thickness of layers. In FE discretization, 150 elements in the length direction and 10 elements in the width direction are used. Fig. 6 shows the representative finite element model for a laminated composite beam in ANSYS®. As seen in Table 2, the present element shows a good agreement with both the experimental and ANSYS® results. The table also shows that the Poisson's effect is more noticeable on the results when it is taken into account. As previously explained, to ignore this effect the barred stiffness coefficients in Eqs. (8) and (9) are replaced by ones in Eq. (5).

Table 3 Non-dimensional fundamental frequencies ($\Omega_1 = \omega\sqrt{\rho L^4/E_2 h^2}$) for bending vibrations of laminated composite beams with different boundary conditions

Beam	*L*/*h* = 10			*L*/*h* = 20			*L*/*h* = 100		
	FEM[a]	Present		FEM	Present		FEM	Present	
		(-)	(+)		(-)	(+)		(-)	(+)
C-F beam									
0	4.560	4.564	4.560	4.931	4.936	4.931	5.070	5.075	5.070
90	1.002	1.002	1.002	1.012	1.012	1.012	1.015	1.016	1.015
[0/90]s	4.178	4.179	4.178	4.597	4.598	4.597	4.758	4.759	4.758
[45/-45]s	1.332	1.962	1.324	1.337	2.004	1.337	1.341	2.018	1.341
C-C beam									
0	17.215	17.218	17.212	25.336	25.346	25.327	31.916	31.938	31.899
90	5.764	5.767	5.761	6.264	6.267	6.260	6.453	6.458	6.450
[0/90]s	14.839	14.838	14.837	22.679	22.677	22.672	29.873	29.867	29.857
[45/-45]s	7.623	10.240	7.616	8.280	12.014	8.280	8.531	12.811	8.526
S-S beam									
0	11.636	11.645	11.635	13.431	13.444	13.430	14.211	14.227	14.210
90	2.771	2.774	2.771	2.829	2.832	2.829	2.849	2.852	2.848
[0/90]s	10.488	10.489	10.488	12.435	12.438	12.434	13.335	13.338	13.333
[45/-45]s	3.752	6.522	3.752	3.834	6.934	3.834	3.861	7.084	3.861

(-) Poisson's effect excluded, (+) Poisson's effect included
[a] Goyal and Kapania (2007)

Table 4 Non-dimensional fundamental frequencies ($\Omega_2 = \sqrt{12}\Omega_1$) for bending vibrations of laminated composite beams with different boundary conditions

Lamina stacking	C-F beam			C-C beam			S-S beam		
	FEM[a]	Present		FEM	Present		FEM	Present	
		(-)	(+)		(-)	(+)		(-)	(+)
[0/30/0]	12.858	12.921	12.858	80.354	80.682	80.310	36.051	36.227	36.042
[0/45/0]	12.792	12.858	12.792	79.902	80.244	79.860	35.840	36.031	35.835
[0/60/0]	12.769	12.821	12.769	79.703	79.972	79.662	35.760	35.909	35.757
[0/90/0]	12.778	12.808	12.777	79.692	79.853	79.651	35.780	35.865	35.777
$[0/90]_2$	8.853	8.861	8.853	55.753	55.776	55.724	26.352	24.839	24.816
[0/±30/0]	12.403	12.709	12.403	77.580	79.387	77.542	34.745	35.595	34.741
[0/±45/0]	12.270	12.457	12.270	76.703	77.852	76.663	34.373	34.917	34.366

(-) Poisson's effect excluded, (+) Poisson's effect included
[a] Goyal and Kapania (2007)

Table 5 Non-dimensional fundamental frequencies ($\Omega_3 = \omega\sqrt{\rho L^4/E_1 h^2}$) for bending vibrations of symmetric angle ply $[\theta/-\theta]_S$ laminated beams with different boundary conditions

Beam	Method	θ						
		0	15	30	45	60	75	90
C-C	Present	4.841	3.958	2.852	1.929	1.628	1.605	1.615
	Analytical[a]	4.841	3.959	2.853	1.929	1.628	1.605	1.615
C-S	Present	3.723	3.009	2.082	1.359	1.137	1.121	1.128
	Analytical	3.723	3.011	2.084	1.359	1.137	1.121	1.128
C-F	Present	0.979	0.729	0.485	0.314	0.263	0.259	0.261
	Analytical	0.979	0.729	0.485	0.314	0.263	0.259	0.261
S-S	Present	2.649	2.307	1.505	0.902	0.736	0.725	0.730
	Analytical	2.649	2.310	1.508	0.902	0.736	0.725	0.730

[a] Jafari-Talookolaei *et al*. (2012)

4.3 Verification with previous results

The first example is taken from Goyal and Kapania (2007) for a laminated composite beam with the geometry and material properties as E_1/E_2 = 25, $G_{12}/E_2 = G_{13}/E_2$ = 0.5, G_{23}/E_2 = 0.2, E_2 = 1.9584×108 psf, ν_{12} = 0.3, ρ = 0.250387 slugs/ft^3, h/b = 0.5, b = 0.1 ft. Three slenderness ratios of L/h = 10, 20, and 100 are considered. The natural frequencies of bending vibrations of the beam for different end conditions and lay-ups are presented in Table 3 with the non-dimensional form of $\Omega_1 = \omega\sqrt{\rho L^4/E_2 h^2}$. It can be seen that the present solutions agree well those of Goyan and Kapania (2007) when the Poisson's effect is included. It should be noted that the Poisson's effect is more noticeable for angle-ply lay-up even though the slenderness ratio increases.

As a second example, the fundamental frequencies with the non-dimensional form of $\Omega_2 = \sqrt{12}\Omega_1$ for bending vibrations of different symmetric and anti-symmetric laminated beams with and without the Poisson's effect are calculated and tabulated in Table 4. Geometry and material properties are taken from Goyal and Kapania (2007) as: E_1/E_2 = 13.7088, G_{12}/E_2 = 0.5471, G_{13}/E_2 = 0.45679, G_{23}/E_2 = 0.269641, E_2 = 9.42512 GPa, ν_{12} = 0.3, ρ = 1550.0666 kg/m^3, h/b = 0.3175, b = 0.01 m, L/h = 60. As can be seen, the present element is in good agreement with that of Goyal and Kapania (2007). As the fibre angle increases, the differences between the present results with and without the Poisson's effect decrease for the symmetric angle-ply laminates and increase for the anti-symmetric ones.

Third example considers the laminated composite beams with different boundary condition and different angle-ply lamina sequences. Geometry and material properties are the same with those used in the convergence study. Natural frequencies are presented in a non-dimensional form as $\Omega_3 = \omega\sqrt{\rho L^4/E_1 h^2}$ in Tables 5 and 6.

In Table 5, non-dimensional fundamental frequencies for bending vibrations of symmetric angle ply $[\theta/-\theta]_S$ laminates obtained by the present method are compared with those of the series load solution in conjunction with Lagrange multipliers given by Jafari-Talookolaei *et al*. (2012). As seen, the results are in excellent agreement.

Table 6 gives the non-dimensional natural frequencies of the laminated beams with anti-symmetric angle-ply $[\pm 45]_2$ lamina stacking and different boundary conditions. Present results are compared with the analytical solution by Jafari

Table 6 The first three non-dimensional fundamental frequencies ($\Omega_3 = \omega\sqrt{\rho L^4/E_1 h^2}$) for bending vibrations of the anti-symmetric angle-ply $[\pm 45]_2$ laminated beams with different boundary conditions

Beam	Method	1st mode	2nd mode	3rd mode
C-C	Present	1.977	5.185	9.587
	Analytical[a]	1.977	5.184	9.585
	IGA[b]	1.976	5.184	9.584
	DQM[c]	1.844	4.987	9.539
	HSDT[d]	1.980	5.216	9.691
S-S	Present	0.901	3.502	7.537
	Analytical	0.901	3.501	7.535
	IGA	0.901	3.500	7.535
	HSDT	0.827	3.233	7.014
C-F	Present	0.323	1.967	5.285
	Analytical	0.323	1.967	5.283

[a] Series solution with Lagrange multipliers by Jafari-Talookolaei *et al*. (2012)
[b] Isogeometric FEM by Wang *et al*. (2015);
[c] State-space-based differential quadrature method by Chen *et al*. (2004);
[d] Higher-order shear deformation theory by Chandrashekhara and Bangera (1992)

Talookolaei *et al*. (2012), isogeometric finite element method by Wang *et al*. (2015), state-space-based differential quadrature method by Chen *et al*. (2004) and the finite element based on a higher-order shear deformation theory by Chandrashekhara and Bangera (1992) for testing the validity of the present method. According to the table, the present element very close results to the analytical ones compared to other methods.

4.4 Parametric study

In this section, the non-dimensional natural frequencies and corresponding mode shapes of laminated composite beams with various configurations are presented. The beams have the slenderness L/h = 10, and cross-sectional dimensions are assumed to be unity. The Poisson's effect is considered. All frequencies are given in the dimensionless form as $\Omega_3 = \omega(L^2/h)\sqrt{\rho/E_1}$. Some new results which can be used a referencing data for future studies are presented. Unless otherwise stated, the material properties of the beam are E_1/E_2 = Open, $G_{12}/E_2 = G_{13}/E_2 = 0.5$, $G_{23}/E_2 = 0.2$, $\nu = 0.3$, $\rho = 1550$ kg/m^3.

Tables 7-9 show the results of laminated composite beams with different lay-ups and boundary conditions (C-C, S-S and F-F) for various orthotropy ratio such as E_1/E_2 = 10, 20, and 40. As seen, for both cross-ply and angle-ply laminates, when the orthotropy ratio increases, the non-

Table 7 Non-dimensional frequencies ($\Omega_3 = \omega\sqrt{\rho L^4/E_1 h^2}$) of cross-ply laminated beams with various end conditions for different orthotropy ratio E_1/E_2 (L/h = 10)

Lay-up	Mode	$E_1/E_2 = 10$			$E_1/E_2 = 20$			$E_1/E_2 = 40$		
		F-F	C-C	S-S	F-F	C-C	S-S	F-F	C-C	S-S
[0/90]	1	3.1513	2.8588	1.4258	2.6551	2.3087	1.2050	2.3097	1.8773	1.0532
	2	7.0248	6.7679	5.0825	4.9673	4.9672	4.1531	3.5124	3.5124	3.4432
	3	7.7034	7.0248	7.0248	6.2672	5.2777	4.9673	5.1553	4.1100	3.5124
	4	13.1008	11.5098	9.5761	9.9347	8.7945	7.7719	7.0249	6.7067	6.2278
	5	14.0497	14.0497	11.2529	10.3416	9.9346	9.8739	8.1703	7.0248	7.0249
[0/90/0]	1	5.5086	4.2676	2.5124	4.9672	3.4257	2.3004	3.5124	2.6178	2.0009
	2	7.0248	7.0248	7.0248	4.9789	4.9672	4.9672	4.2547	3.5124	3.5124
	3	11.8530	9.1669	7.9853	9.6189	7.0397	6.5576	7.0248	5.2563	5.1012
	4	14.0497	14.0497	13.1808	9.9346	9.9346	9.9346	7.4024	7.0248	7.0248
	5	18.4587	14.8303	14.0497	14.2652	11.1671	10.9433	10.5375	8.2073	8.1386
$[0/90]_2$	1	4.0823	3.4478	1.8506	3.7095	2.8545	1.6942	3.2974	2.2684	1.5244
	2	7.0248	7.0248	6.3106	4.9672	4.9672	4.9672	3.5124	3.5124	3.5124
	3	9.4589	7.7700	7.0248	7.9265	6.1053	5.3393	6.3666	4.6586	4.3388
	4	14.0497	12.8514	11.3007	9.9346	9.8602	9.4070	7.0248	7.0248	7.0248
	5	15.4342	14.0497	12.0456	12.2819	9.9346	9.9346	9.4320	7.3888	7.2368
$[0/90]_S$	1	5.2541	4.0368	2.3982	4.7225	3.2246	2.1841	3.5124	2.4569	1.8912
	2	7.0248	7.0248	7.0248	4.9672	4.9672	4.9672	4.0169	3.5124	3.5124
	3	11.2221	8.6373	7.5666	9.0593	6.6126	6.1807	6.9497	4.9294	4.7919
	4	14.0497	13.9501	11.6847	9.9346	9.9346	9.9346	7.0248	7.0248	7.0248
	5	17.4050	14.0497	13.3565	13.4017	10.4782	10.2794	9.9865	7.6902	7.6291

Table 8 Non-dimensional frequencies ($\Omega_3 = \omega\sqrt{\rho L^4/E_1 h^2}$) of angle-ply laminated beams with various end conditions for different orthotropy ratio E_1/E_2 (L/h = 10)

Lay-up	Mode	E_1/E_2=10			E_1/E_2=20			E_1/E_2=40		
		F-F	C-C	S-S	F-F	C-C	S-S	F-F	C-C	S-S
					$[\theta/-\theta]_2$					
30	1	3.7253	3.3092	1.6817	3.0561	2.6098	1.3832	2.4081	1.9867	1.0926
	2	9.0202	7.7588	5.9974	7.1584	5.9361	4.7769	5.4759	4.4164	3.6663
	3	13.0994	13.0994	9.9093	11.7953	9.8646	8.2946	8.8273	7.2557	6.6264
	4	15.2823	13.1164	11.6825	12.3513	12.3513	9.0295	11.5680	10.2584	6.7645
	5	20.6728	18.9228	13.5814	16.4769	14.0623	12.9268	12.1405	11.5680	9.9685
45	1	2.5212	2.3668	1.1345	1.8473	1.7249	0.8315	1.3356	1.2428	0.6013
	2	6.3869	5.8434	4.2263	4.6596	4.2352	3.0847	3.3594	3.0405	2.2246
	3	11.3103	10.2354	6.4763	8.2141	7.3871	4.7454	5.9046	5.2892	3.4279
	4	12.5565	12.5565	8.6292	9.3848	9.3848	6.2680	6.8212	6.8212	4.5062
	5	15.5570	15.1513	13.7758	12.1270	10.9001	9.9617	8.6939	7.7889	7.1412
60	1	2.0593	1.9548	0.9262	1.4571	1.3830	0.6553	1.0308	0.9784	0.4636
	2	5.2634	4.8840	3.4798	3.7240	3.4551	2.4620	2.6344	2.4440	1.7417
	3	9.4112	8.6360	5.2317	6.6581	6.1091	3.7005	4.7098	4.3211	2.6172
	4	10.4324	10.4324	7.1778	7.3933	7.3933	5.0781	5.2321	5.2321	3.5921
	5	13.5095	12.8782	11.5705	9.9609	9.1094	8.1851	7.0458	6.4430	5.7897
					$[\theta/-\theta]_S$					
30	1	3.3756	3.0834	1.6927	2.7598	2.4356	1.3876	2.2200	1.8856	1.0935
	2	8.2827	7.3303	5.4603	6.5997	5.6366	4.3723	5.1576	4.2560	3.4364
	3	12.7622	12.5013	10.0553	10.8015	9.4573	8.3856	8.3996	7.0452	6.5065
	4	14.5338	12.9390	10.9676	12.0766	11.7095	8.5393	10.7922	10.0050	6.6703
	5	20.1106	18.1635	12.3728	15.6287	13.5923	10.9907	11.7395	10.7284	9.4333
45	1	2.4421	2.3052	1.1368	1.7989	1.6874	0.8322	1.3121	1.2246	0.6014
	2	6.2039	5.7143	4.1001	4.5506	4.1587	3.0102	3.3073	3.0041	2.1892
	3	10.9950	10.0404	6.4921	8.0412	7.2745	4.7531	5.8249	5.2365	3.4311
	4	12.9841	12.9841	8.4342	9.5061	9.5061	6.1545	6.8622	6.8622	4.4527
	5	13.2656	13.2187	12.7314	11.9114	10.7559	9.7438	8.5954	7.7228	7.0549
60	1	2.0509	1.9480	0.9264	1.4528	1.3796	0.6554	1.0290	0.9769	0.4636
	2	5.2436	4.8695	3.4662	3.7141	3.4478	2.4553	2.6301	2.4408	1.7388
	3	9.3768	8.6137	5.2332	6.6420	6.0979	3.7011	4.7030	4.3163	2.6175
	4	10.4664	10.4664	7.1562	7.4022	7.4022	5.0674	5.2349	5.2349	3.5876
	5	11.5043	11.4998	11.3466	9.9399	9.0949	8.1647	7.0369	6.4368	5.7820

Table 9 Non-dimensional frequencies ($\Omega_3 = \omega\sqrt{\rho L^4/E_1 h^2}$) of unsymmetric laminated beams with various end conditions for different orthotropy ratio E_1/E_2 (L/h = 10)

Lay-up	Mode	E_1/E_2=10			E_1/E_2=20			E_1/E_2=40		
		F-F	C-C	S-S	F-F	C-C	S-S	F-F	C-C	S-S
					$[\theta/-\theta]_2$					
30	1	3.7884	3.4203	1.8578	3.0803	2.6935	1.5497	2.5562	2.1228	1.2961
	2	9.0361	7.8864	5.8893	7.1505	6.0149	4.6317	5.7027	4.5874	3.7123
	3	9.0840	8.9985	8.9643	7.1601	7.0978	7.0435	5.7067	5.6539	5.5696
	4	15.3445	13.2944	11.3589	11.8260	9.9750	8.9260	9.1575	7.4914	6.9546
	5	17.7096	17.6819	12.5303	13.7819	13.7906	11.0756	10.8193	10.5570	9.6712

Table 9 Continued

Lay-up	Mode	E_1/E_2=10			E_1/E_2=20			E_1/E_2=40		
		F-F	C-C	S-S	F-F	C-C	S-S	F-F	C-C	S-S
		$[\theta/-\theta]_2$								
45	1	3.3755	3.0726	1.5703	2.7997	2.4558	1.3078	2.3986	1.9812	1.1203
	2	8.2389	7.2573	5.4104	6.6225	5.6145	4.3599	5.1581	4.3507	3.5804
	3	8.8447	8.8304	8.7937	6.7681	6.7550	6.7329	5.4027	5.1477	5.1350
	4	14.0380	12.3351	10.2446	10.9832	9.3686	8.2449	8.6388	7.1224	6.5699
	5	17.5443	17.5700	11.7685	13.3933	13.3970	10.3045	10.1981	10.0463	9.0011
60	1	3.2071	2.9200	1.4558	2.6913	2.3540	1.2247	2.3355	1.9146	1.0667
	2	7.8581	6.9297	5.1793	5.8948	5.3988	4.2206	4.2990	4.2020	3.4970
	3	8.0350	8.0335	8.0312	6.3789	5.8945	5.8944	5.2475	4.3045	4.3008
	4	13.3980	11.8056	9.7589	10.5644	9.0166	7.9253	8.3548	6.8814	6.3608
	5	16.0572	16.0573	11.4032	11.7803	11.7791	9.9943	8.5914	8.5902	8.5863
		$[\theta/-\theta]_S$								
30	1	3.1936	2.9300	1.4390	2.5567	2.2868	1.1537	2.0523	1.7786	0.9280
	2	7.9414	7.0704	5.2652	6.2261	5.3931	4.1371	4.8674	4.0891	3.2436
	3	9.5108	9.5108	8.6637	7.9852	7.9852	7.1855	7.0409	6.8347	5.9821
	4	13.7969	12.1784	10.5345	10.6033	9.1499	8.1036	8.1010	7.0409	6.1983
	5	19.0217	17.8039	11.6387	15.1942	13.2335	9.9392	11.4008	9.7827	8.4868
45	1	2.3844	2.2558	1.0726	1.7527	1.6494	0.7886	1.2843	1.2023	0.5780
	2	6.0782	5.6156	4.0195	4.4488	4.0827	2.9433	3.2463	2.9600	2.1486
	3	10.0238	9.9003	6.3632	7.8948	7.1655	4.6768	5.7352	5.1733	3.3949
	4	10.8360	10.0238	8.2653	8.0375	8.0375	6.0228	6.2886	6.2886	4.3761
	5	14.6862	14.6862	11.2906	11.6768	10.6233	9.6350	8.4845	7.6451	6.9698
60	1	2.0444	1.9424	0.9194	1.4486	1.3760	0.6515	1.0267	0.9750	0.4617
	2	5.2293	4.8580	3.4569	3.7044	3.4403	2.4489	2.6250	2.4369	1.7354
	3	9.3576	8.5971	5.2214	6.6274	6.0868	3.6952	4.6950	4.3104	2.6149
	4	9.7018	9.7018	7.1367	7.2457	7.2457	5.0546	5.1925	5.1925	3.5808
	5	11.0895	11.0895	10.2595	8.9759	8.9759	8.1526	7.0266	6.4293	5.7740

dimensional natural frequencies decrease. F-F beam has the greatest natural frequencies compared to the others. According to Tables 8 and 9, for angle-ply laminates, the non-dimensional frequencies decrease with increasing the fibre angle.

In Figs. 7-9, the first five mode shapes of vibration for unsymmetric cross-ply, antisymmetric and unsymmetric angle-ply laminated composite beams with C-C, S-S and F-F boundary conditions and the orthotropy ratio E_1/E_2 = 40 are presented to show the effect of material coupling among the displacement components of motion. As seen in Fig. 7, for [0/90] unsymmetric cross-ply laminated beams, bending and torsional vibration components are dominant in the lowest modes. For the lower modes considered, bending-torsion coupling does not appear; however, a small amount of extension-bending coupling is observed. According to Fig. 8, for [45/-45] antisymmetric angle-ply laminated beams, bending modes of vibration are generally observed, and there is no coupling between the bending and torsional components. In some modes, e.g., 3rd mode of S-S beam, 4th mode of F-F and C-C beams, the extensional and torsional components are greatly coupled. For [0/45] unsymmetric angle-ply laminated beams, as can be seen in Fig. 9, the mode shapes show great complexity and involve various couplings among the extensional, bending and torsional components of the motion.

5. Conclusions

This study presents a finite element model with five nodes and 13 DOFs for free vibration analysis of laminated composite beams with arbitrary lay-ups using the first-order shear deformation theory. The model considers simultaneously the material couplings among extensional, bending and torsional deformations due to anisotropy and the Poisson's effect. Applying Lagrange's principle gives the equations of motion and thus element matrices of the laminated composite beam. The free vibration problem is solved as a standard eigenvalue problem to obtain the natural frequencies and corresponding mode shapes. The current element is verified by comparing with experimental study, the results reported in the literature as well as those obtained by ANSYS® finite element analysis software to show its accuracy. Some parametric results can be used for benchmarking for the future studies.

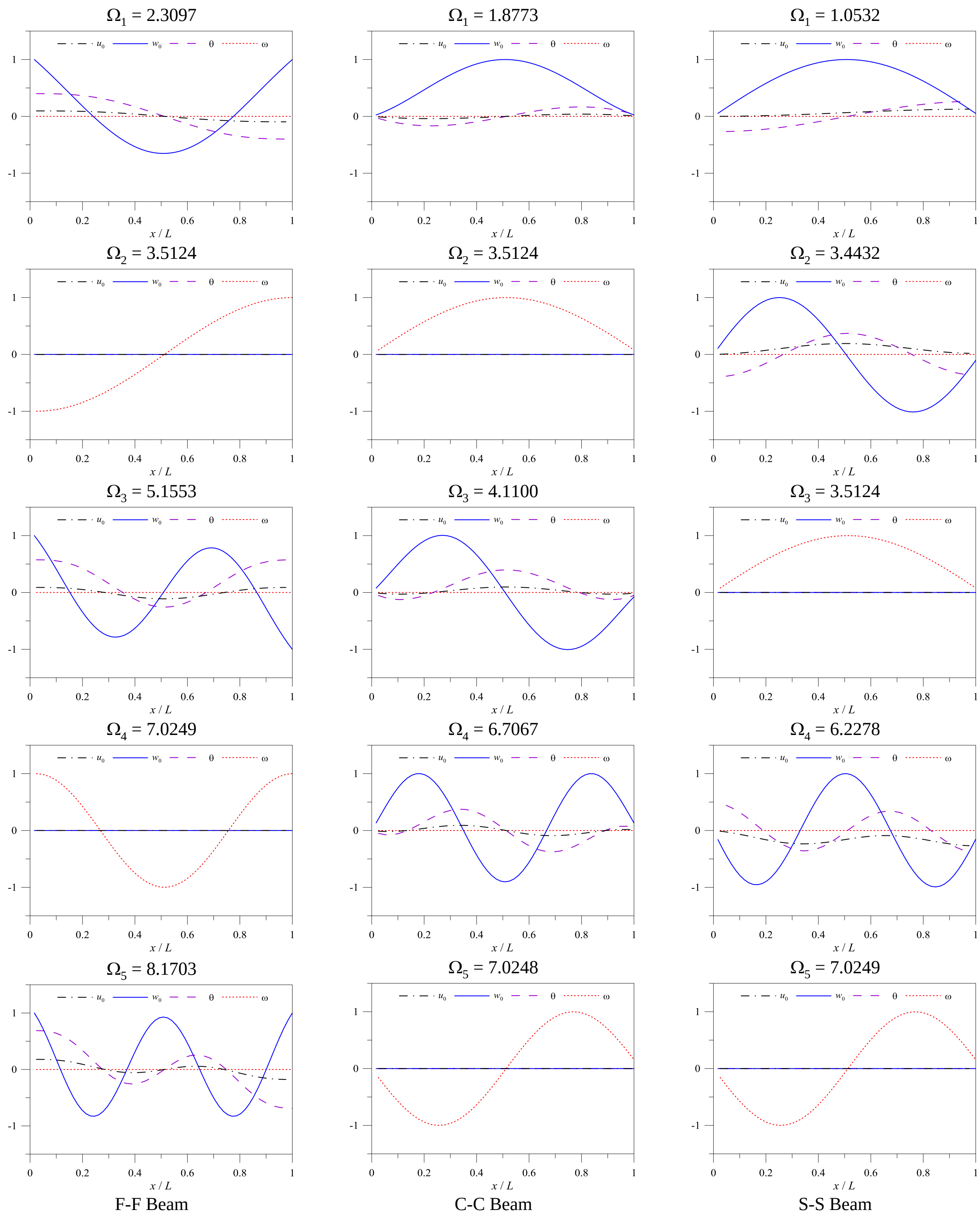

Fig. 7 The lowest five mode shapes of [0/90] unsymmetric cross-ply laminated composite beams with $L/h=10$ and $E_1/E_2=40$

The present element can capture vibration modes of the laminated composite beams in a good accuracy. According to the study, for unsymmetric angle-ply laminated beams, the material coupling greatly affects the vibration modes.

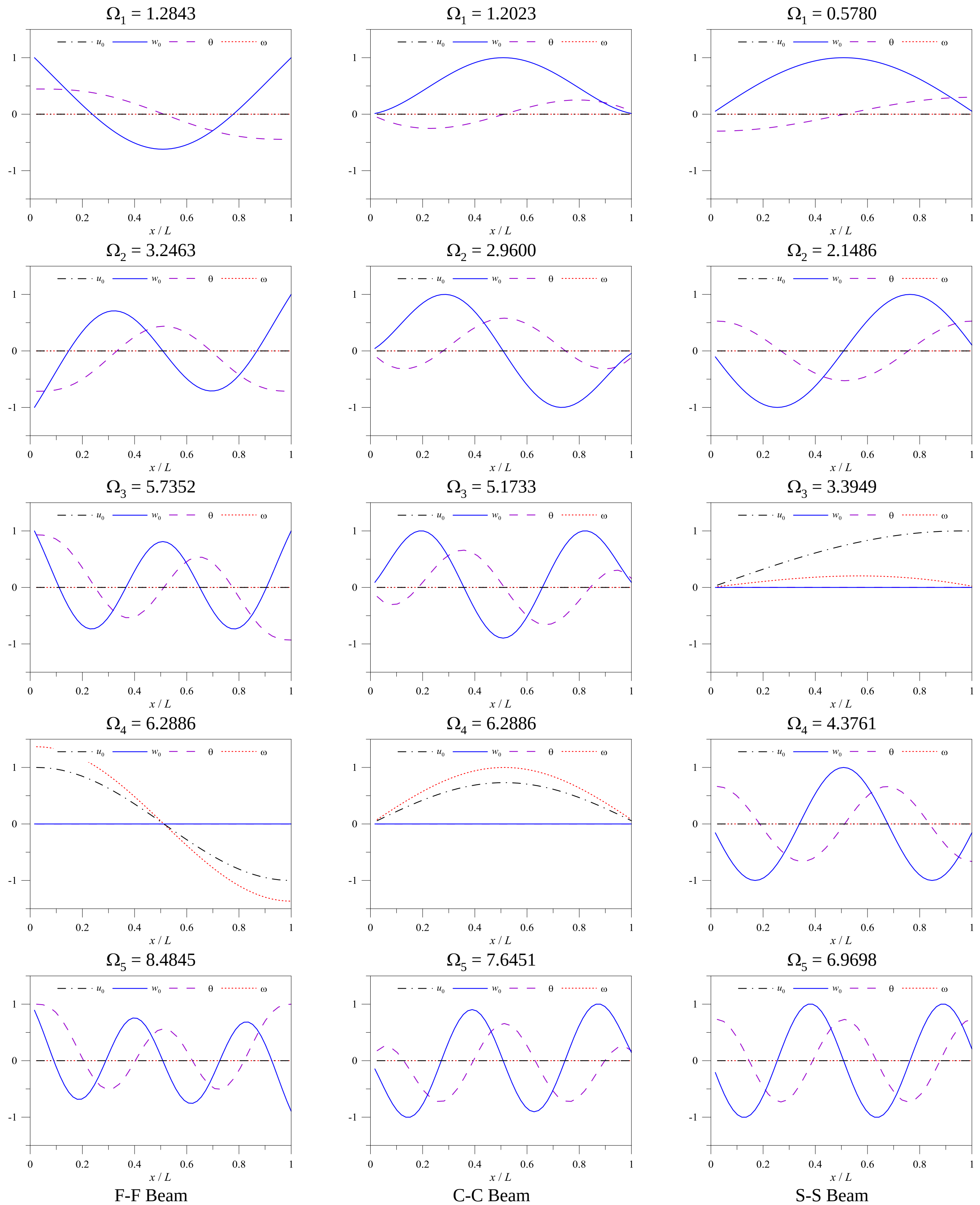

Fig. 8 The lowest five mode shapes of [45/-45] antisymmetric angle-ply laminated composite beams with L/h = 10 and E_1/E_2 = 40

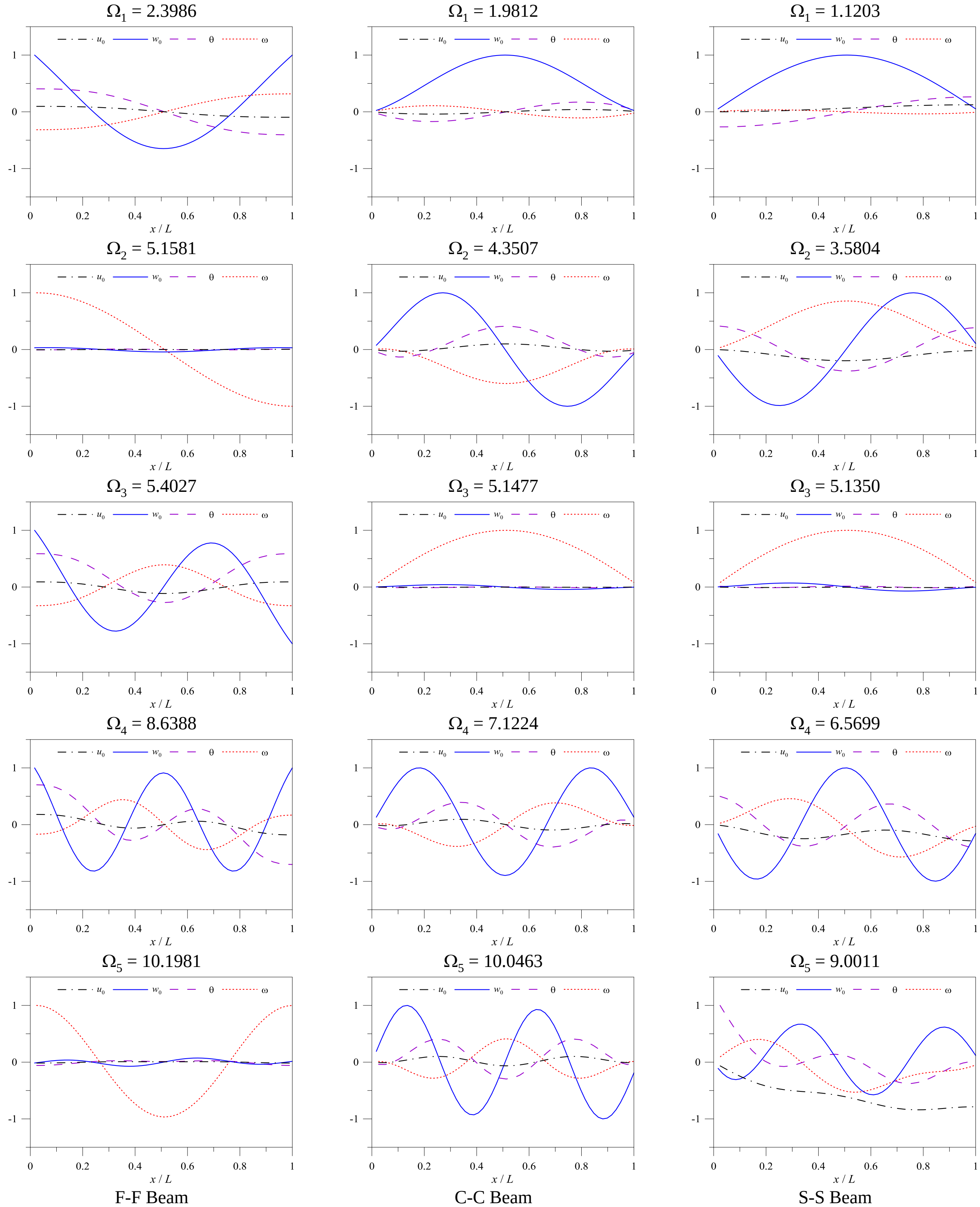

Fig. 9 The lowest five mode shapes of [0/45] unsymmetric angle-ply laminated composite beams with L/h = 10 and E_1/E_2 = 40

References

ANSYS (2014), Mechanical APDL Release 16.0.

Chakraborty, A., Roy Mahapatra, D. and Gopalakrishnan, S. (2002), "Finite element analysis of free vibration and wave propagation in asymmetric composite beams with structural discontinuities", *Compos. Struct.*, **55**, 23-36. https://doi.org/10.1016/S0263-8223(01)00130-1

Chalak, H.D., Chakrabarti, A., Iqbal, M.A. and Sheikh, A.H. (2012), "Vibration of laminated sandwich beams having soft core", *J. Vib. Control*., **18**, 1422-1435. https://doi.org/10.1177/1077546311421947

Chandrashekhara, K. and Bangera, K.M. (1992), "Free vibration of composite beams using a refined shear flexible beam element", *Comput. Struct.*, **43**, 719-727. https://doi.org/10.1177/1077546311421947

Chen, W.Q., Lv, C.F. and Bian, Z.G. (2004), "Free vibration analysis of generally laminated beams via state-space-based differential quadrature", *Compos. Struct.*, **63**, 417-425. https://doi.org/10.1016/S0263-8223(03)00190-9

Filippi, M. and Carrera, E. (2016), "Bending and vibrations analyses of laminated beams by using a zig-zag-layer-wise theory", *Compos. Part B Eng*., **98**, 269-280. https://doi.org/10.1016/j.compositesb.2016.04.050

Goyal, V.K. and Kapania, R.K. (2007), "A shear-deformable beam element for the analysis of laminated composites", *Finite Elem. Anal. Des*., **43**, 463-477. https://doi.org/10.1016/j.finel.2006.11.011

Jafari-Talookolaei, R.A., Abedi, M., Kargarnovin, M.H. and Ahmadian, M.T. (2012), "An analytical approach for the free vibration analysis of generally laminated composite beams with shear effect and rotary inertia", *Int. J. Mech. Sci*., **65**, 97-104. https://doi.org/10.1016/j.ijmecsci.2012.09.007

Jafari-Talookolaei, R.A., Abedi, M. and Attar, M. (2017), "In-plane and out-of-plane vibration modes of laminated composite beams with arbitrary lay-ups", *Aerosp. Sci. Technol*., **66**, 366-379. https://doi.org/10.1016/j.ast.2017.02.027

Jun, L., Hongxing, H. and Rongying, S. (2008), "Dynamic finite element method for generally laminated composite beams", *Int. J. Mech. Sci*., **50**, 466-480. https://doi.org/10.1016/j.ijmecsci.2007.09.014

Kadivar, M.H. and Mohebpour, S.R. (1998), "Finite element dynamic analysis of unsymmetric composite laminated beams with shear effect and rotary inertia under the action of moving loads", *Finite Elem. Anal. Des*. **29**, 259-273. https://doi.org/10.1016/S0168-874X(98)00024-9

Kahya, V. (2012), "Dynamic analysis of laminated composite beams under moving loads using finite element method", *Nucl. Eng. Des.*, **243**, 41-48. https://doi.org/10.1016/j.nucengdes.2011.12.015

Kahya, V. and Turan, V. (2018), "Vibration and buckling of laminated beams by a multi-layer finite element model", *Steel Compos. Struct., Int. J.*, **28**(4), 415-426. https://doi.org/10.12989/scs.2018.28.4.415

Lezgy-Nazargah, M., Shariyat, M. and Beheshti-Aval, S.B. (2011), "A refined high-order global-local theory for finite element bending and vibration analyses of laminated composite beams", *Acta Mech*., **217**, 219-242. https://doi.org/10.1007/s00707-010-0391-9

Mohebpour, S.R., Fiouz, A.R. and Ahmadzadeh, A.A. (2011), "Dynamic investigation of laminated composite beams with shear and rotary inertia effect subjected to the moving oscillators using FEM", *Compos. Struct*., **93**, 1118-1126. https://doi.org/10.1016/j.compstruct.2010.09.011

OMA (2006), Operational Modal Analysis Software.

PULSE (2006), Analysers and Solutions.

Ramtekkar, G.S., Desai, Y.M. and Shah, A.H. (2002), "Natural vibrations of laminated composite beams by using mixed finite element modelling", *J. Sound Vib*., **257**, 635-651. https://doi.org/10.1006/jsvi.2002.5072

Reddy, J.N. (1997), *Mechanics of Laminated Composite Plates and Shells*: *Theory and Analysis*, CRC Press, Boca Raton, FL, USA.

Sayyad, A.S. and Ghugal, Y.M. (2017), "Bending, buckling and free vibration of laminated composite and sandwich beams: A critical review of literature", *Compos. Struct.*, **171**, 486-504. https://doi.org/10.1016/j.compstruct.2017.03.053

Shao, D., Hu, S., Wang, Q. and Pang, F. (2017), "Free vibration of refined higher-order shear deformation composite laminated beams with general boundary conditions", *Compos. Part B Eng*., **108**, 75-90. https://doi.org/10.1016/j.compositesb.2016.09.093

Shi, G. and Lam, K.Y. (1999), "Finite element vibration analysis of composite beams based on higher-order beam theory", *J. Sound Vib.*, **219**, 707-721. https://doi.org/10.1006/jsvi.1998.1903

Subramanian, P. (2006), "Dynamic analysis of laminated composite beams using higher order theories and finite elements", *Compos. Struct*., **73**, 342-353. https://doi.org/10.1016/j.compstruct.2005.02.002

Vidal, P. and Polit, O. (2010), "Vibration of multilayered beams using sinus finite elements with transverse normal stress", *Compos. Struct*., **92**, 1524-1534. https://doi.org/10.1016/j.compstruct.2009.10.009

Vo, T.P. and Thai, H.T. (2012a), "Free vibration of axially loaded rectangular composite beams using refined shear deformation theory", *Compos. Struct*., **94**, 3379-3387. https://doi.org/10.1016/j.compstruct.2012.05.012

Vo, T.P. and Thai, H.T. (2012b), "Vibration and buckling of composite beams using refined shear deformation theory", *Int. J. Mech. Sci*., **62**, 67-76. https://doi.org/10.1016/j.ijmecsci.2012.06.001

Vo, T.P., Thai, H.T. and Inam, F. (2013), "Axial-flexural coupled vibration and buckling of composite beams using sinusoidal shear deformation theory", *Arch. Appl. Mech*., **83**, 605-622. https://doi.org/10.1007/s00419-012-0707-4

Vo, T.P., Thai, H.T. and Aydogdu, M. (2017), "Free vibration of axially loaded composite beams using a four-unknown shear and normal deformation theory", *Compos. Struct*., **178**, 406-414. https://doi.org/10.1016/j.compstruct.2017.07.022

Wang, X., Zhu, X. and Hu, P. (2015), "Isogeometric finite element method for buckling analysis of generally laminated composite beams with different boundary conditions", *Int. J. Mech. Sci.*, **104**, 190-199. https://doi.org/10.1016/j.ijmecsci.2015.10.008

Wimmer, H. and Gherlone, M. (2017), "Explicit matrices for a composite beam-column with refined zigzag kinematics", *Acta Mech.*, **228**, 2107-2117. https://doi.org/10.1007/s00707-017-1816-5

CC

Appendix

The shape functions for the present finite element model are

$$\begin{aligned} \Phi_1 &= (1-\xi)(1-2\xi), \\ \Phi_2 &= 4\xi(1-\xi), \\ \Phi_3 &= -\xi(1-2\xi), \\ \Psi_1 &= \frac{1}{2}(1-\xi)(1-3\xi)(2-3\xi), \\ \Psi_2 &= \frac{9}{2}\xi(1-\xi)(2-3\xi), \\ \Psi_3 &= -\frac{9}{2}\xi(1-\xi)(1-3\xi), \\ \Psi_4 &= \frac{1}{2}\xi(1-3\xi)(2-3\xi) \end{aligned} \tag{A1}$$

where $\xi = x/l$ and l is the element length.

The element mass and stiffness matrices are in the form

$$\boldsymbol{M}_e = \begin{bmatrix} \boldsymbol{m}_{11} & \boldsymbol{0} & \boldsymbol{m}_{13} & \boldsymbol{0} \\ \boldsymbol{0} & \boldsymbol{m}_{22} & \boldsymbol{0} & \boldsymbol{0} \\ \boldsymbol{m}_{13}^T & \boldsymbol{0} & \boldsymbol{m}_{33} & \boldsymbol{0} \\ \boldsymbol{0} & \boldsymbol{0} & \boldsymbol{0} & \boldsymbol{m}_{44} \end{bmatrix}_{13\times13}, \quad \boldsymbol{K}_e = \begin{bmatrix} \boldsymbol{k}_{11} & \boldsymbol{0} & \boldsymbol{k}_{13} & \boldsymbol{k}_{14} \\ \boldsymbol{0} & \boldsymbol{k}_{22} & \boldsymbol{k}_{23} & \boldsymbol{0} \\ \boldsymbol{k}_{13}^T & \boldsymbol{k}_{23}^T & \boldsymbol{k}_{33} & \boldsymbol{k}_{34} \\ \boldsymbol{k}_{14}^T & \boldsymbol{0} & \boldsymbol{k}_{34}^T & \boldsymbol{k}_{44} \end{bmatrix}_{13\times13} \tag{A2}$$

where

$$\begin{aligned} \boldsymbol{m}_{11} &= \frac{I_0 l}{15}\begin{bmatrix} 4 & 2 & -1 \\ & 16 & 2 \\ \text{Sym.} & & 4 \end{bmatrix}, \\ \boldsymbol{m}_{13} &= \frac{I_1 l}{15}\begin{bmatrix} 4 & 2 & -1 \\ & 16 & 2 \\ \text{Sym.} & & 4 \end{bmatrix}, \\ \boldsymbol{m}_{22} &= I_0 l\begin{bmatrix} \frac{16}{105} & \frac{33}{280} & -\frac{3}{70} & \frac{19}{840} \\ & \frac{27}{35} & -\frac{27}{280} & -\frac{3}{70} \\ & & \frac{27}{35} & \frac{33}{280} \\ \text{Sym.} & & & \frac{16}{105} \end{bmatrix}, \\ \boldsymbol{m}_{33} &= \frac{I_2 l}{15}\begin{bmatrix} 4 & 2 & -1 \\ & 16 & 2 \\ \text{Sym.} & & 4 \end{bmatrix}, \\ \boldsymbol{m}_{44} &= \frac{I_2 l}{15}\begin{bmatrix} 4 & 2 & -1 \\ & 16 & 2 \\ \text{Sym.} & & 4 \end{bmatrix} \end{aligned} \tag{A3}$$

$$\begin{aligned} \boldsymbol{k}_{11} &= \frac{\bar{A}_{11}}{3l}\begin{bmatrix} 14 & -16 & 2 \\ & 32 & -16 \\ \text{Sym.} & & 14 \end{bmatrix}, \\ \boldsymbol{k}_{13} &= \frac{\bar{B}_{11}}{3l}\begin{bmatrix} 14 & -16 & 2 \\ & 32 & -16 \\ \text{Sym.} & & 14 \end{bmatrix}, \\ \boldsymbol{k}_{14} &= \frac{\bar{B}_{16}}{3l}\begin{bmatrix} 14 & -16 & 2 \\ & 32 & -16 \\ \text{Sym.} & & 14 \end{bmatrix}, \\ \boldsymbol{k}_{22} &= \frac{\bar{A}_{55}}{5l}\begin{bmatrix} 37 & -\frac{189}{4} & \frac{27}{2} & -\frac{13}{4} \\ & 108 & -\frac{297}{4} & \frac{27}{2} \\ & & 108 & -\frac{189}{4} \\ \text{Sym.} & & & 37 \end{bmatrix}, \\ \boldsymbol{k}_{23} &= \bar{A}_{55}\begin{bmatrix} -\frac{83}{60} & -\frac{11}{15} & \frac{7}{60} \\ \frac{33}{20} & -\frac{9}{5} & \frac{3}{20} \\ -\frac{3}{20} & \frac{9}{5} & -\frac{33}{20} \\ -\frac{7}{60} & \frac{11}{15} & \frac{83}{60} \end{bmatrix}, \\ \boldsymbol{k}_{33} &= \frac{\bar{D}_{11}}{3l}\begin{bmatrix} 14 & -16 & 2 \\ & 32 & -16 \\ \text{Sym.} & & 14 \end{bmatrix} + \frac{\bar{A}_{55} l}{15}\begin{bmatrix} 4 & 2 & -1 \\ & 16 & 2 \\ \text{Sym.} & & 4 \end{bmatrix}, \\ \boldsymbol{k}_{34} &= \frac{\bar{D}_{16}}{3l}\begin{bmatrix} 14 & -16 & 2 \\ & 32 & -16 \\ \text{Sym.} & & 14 \end{bmatrix}, \\ \boldsymbol{k}_{44} &= \frac{\bar{D}_{66}}{3l}\begin{bmatrix} 14 & -16 & 2 \\ & 32 & -16 \\ \text{Sym.} & & 14 \end{bmatrix} \end{aligned} \tag{A4}$$

where the stiffness and inertia coefficients are given by Eqs. (5), (8) and (9), respectively.